View metadata, citation and similar papers at core.ac.uk
brought to you by CORE
provided by Northumbria Research Link

The Efficient Denoising Artificial Light Interference using Discrete Wavelet Transform with Application to Indoor Optical Wireless System

S. Rajbhandari*, Prof. Z. Ghassemlooy*, and Prof. M. Angelova**
*Optical Communications Research Group, School of CEIS, Northumbria University, UK
** Intelligent Modelling Lab, School of CEIS, Northumbria University, UK
School of CEIS, Northumbria University, UK
sujan.rajbhandari@unn.ac.uk, fary.ghassemlooy@unn.ac.uk, maia.angelova@unn.ac.uk

***Abstract*—**Reducing the effect of the artificial light interference (ALI) in indoor optical wireless (OW) communication is a challenging prospect because of the spectral overlaps between the interference and the baseband modulating signal. High pass filtering is used for mitigating the effect of ALI; however it introduces another form of interference known as baseline wander (BLW). In this paper, an alternative approach is investigation to minimize the performance degradation due to ALI using the discrete wavelet transform (DWT). Performances of different digital baseband modulation techniques are examined under the influence of the ALI in line-of-sight (LOS) links and we show that the DWT is very effective in reducing the effect of the ALI.

Index Terms—Optical wireless communication, discrete wavelet transform, denoising

1. Introduction

We have seen an exponential growth in bandwidth requirement per end-user due to profuse growth in the internet user and the file sharing, and video broadcasting. Though RF technologies already available can provide the required bandwidth up to a certain point beyond which bandwidth congestion becomes a bottleneck. One of the proposed solutions is to move to a higher frequency band of 10 GHZ and 60 GHz, which is still in research and development stages. However, there is a solution to the last-mile problem that is based on the optical communication systems. Though the fibre-to-the-home is already a proven concept, the cost and environmental effect may count against it for new installations. The alternative solutions would be to use OW links, which is more suitable for indoor as well as outdoor applications. Outdoor OW link is more mature than the indoor offering data rates of 10 Gbps per wavelength over a range of up to 6 km [1, 2]. The LOS indoor OW systems can provide data rates in access of the 1 Gbps without any multiple access [3], but high blocking probability and lack of mobility make them suitable for limited applications. The diffuse links on the other hand provide mobility to certain extent at the cost of a high path loss and reduce data rates. However, the key challenge to the reliability of the link for both LOS and non-LOS links arises from the ambient light radiations from natural and artificial sources. The background radiation can be received as an average power much larger than the desired signal, even when optical filtering is employed. The background radiation can be model as the signal independent additive white Gaussian noise (AWGN). However, ALIs are periodic and have potential to degrade the performance severely. Fluorescent lamps (FLs) emit strongly at spectral lines 780–950 nm bands. Electronic ballasts driven FLs have electrical spectrum contents that range up to MHz making such lamps potentially a serious impairment to OW links [4-6].

The potential solution to reduce the effect of the fluorescent light interference (FLI) is to use a high pass filter (HPF). Selections of modulation techniques also affect the link performance in presence of FLI [7]. The modulation scheme like pulse position modulation (PPM) with a low spectral content at or near DC level provides immunity to the FLI. On the other hand, on-off keying (OOK) with a high spectral content near DC region is more likely to be affect by the FLI and the power penalty without HPF would be much higher. Digital HPFs provide improved performance compared to its analogue counterpart. However, HPF introduce another type of intersymbol interference (ISI) known as the BLW that mainly affect modulation techniques with strong frequency components at/near the DC region [6, 8]. In this paper, we introduce an alternative approach to HPF to reduce the effect of the FLI using the DWT. In DWT based denoising scheme, the signal is separated into different frequency bands to ensure that interference and modulating signal are effectively separated. Band of frequencies corresponding to the interference are remove from the signal and hence the reconstructed signal in theory can be free from FLI. Since the spectral content of the FLI and modulating signal overlaps for baseband modulation, there would certainly be power penalty compared to ideal channel. It is expected that the

power penalty corresponding to the signal with a low DC component would be much lower. Hence three modulation techniques OOK, PPM and digital pulse interval modulation (DPIM) are studied and their power penalty due to FLI is simulated when employing the DWT for denoising and results are presented.

The paper is organised as follows: a brief overview of the modulation techniques under study is given in Section II, followed by introduction to the ALI and the link error performance in Section III. The concept of the DWT denoising using multiresolutional analysis is given in Section IV. The proposed system is introduced in Section V. Results of computer simulation together with simulation parameters and brief discussions are presented in Section VI. Finally concluding remarks are given in Section VII.

2. Digital Baseband Modulation Techniques for Indoor OW

A number of baseband modulation techniques had been proposed and studied, however this studied is limited to some of the most popular modulation techniques for intensity modulation direct detection (IM/DD) for indoor OW communication namely OOK, PPM and DPIM. Only a brief introduction of these modulation techniques would be provided, for detail information refer to references provided in the respective sections.

A. OOK

The most widely used modulation technique for IM/DD in OW communications is the OOK. This is apparently due to its simplicity and low system complexity. For a nor-return-to-zero (NRZ) OOK scheme, a binary bit 'one' is represented by an optical pulse that occupies the entire bit duration while a bit zero is represented by the absence of an optical pulse (Fig.1). OOK-NRZ provides a good compromise between the power requirement and bandwidth requirement [4] and proves to be very effective scheme in dispersive channels. For distortionless channels, the maximum-likelihood (ML) receiver for OOK with AWGN consists of a continuous-time filter matched to the transmitted pulse shape, followed by a sampler and threshold detector set at midway between the zero bit and one bit energies. The probability of bit error P_{be_OOK} for OOK-NRZ in AWGN channel is given by [9]:

$$P_{be\_OOK} = Q\left(\frac{RP_{avg}\sqrt{T_b}}{\sqrt{N_0/2}}\right), \quad (1)$$

where R is the responsivity of photodiode, P_{avg} is the average transmitted power, $T_b = {R_b}^{-1}$ is the bit durations, R_b is the bit rate, $N_0/2$ is the double-sided noise power spectral density (PSD) and $Q(.)$ is the error function defined as:

$$Q(\varphi) = \frac{1}{\sqrt{2\pi}}\int_{\varphi}^{\infty} e^{(-\omega^2/2)}\, d\omega. \quad (2)$$

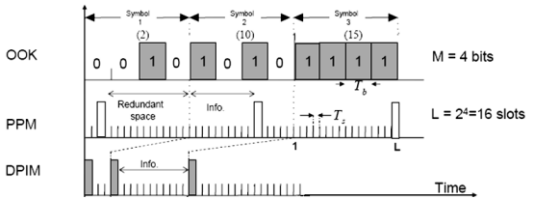

Fig.1. Symbol mapping of OOK, PPM and DPIM.

B. PPM

PPM is an orthogonal baseband modulation technique well investigated in optical communications for its superior power efficiency compared to any other baseband modulation techniques. An L-PPM symbol consists of a single pulse of one slot duration within L ($= 2^{M,}$ where $M > 0$ is an integer) possible time slots with the remaining slots being empty (see Fig.1 for the symbol mapping). The position of the pulse corresponds to the decimal value of the M-bit input data. In order to achieve the same throughput, PPM pulse duration is shorter than the OOK pulse duration by a factor of L_{PPM}/M, where $L_{PPM} = 2^M$ is the slot length of PPM symbol. Hence slot duration of PPM T_{s_PPM} is given by:

$$T_{s\_PPM} = \frac{T_b M}{L_{PPM}}, \quad (3)$$

where $T_b = {R_b}^{-1}$ and R_b is the bit rate.

For distortionless AWGN channel, the slot error probability of L-PPM P_{se_PPM} with a matched filter and a threshold level at the receiver set midway between the low and high energies is given as [9, 10]:

$$P_{se\_PPM} = Q\left(\sqrt{\frac{1}{2}L_{PPM}M}\,\frac{RP_{avg}\sqrt{T_b}}{\sqrt{N_0/2}}\right). \quad (4)$$

From (1), (3) and (4), it is apparent that the PPM system provides the power efficiency at the cost of bandwidth by a factor of L_{PPM}/M compared to OOK. To achieve similar error performance, the average power required by the PPM is lower than that required by OOK by a factor of $\sqrt{0.5L_{PPM}M}$. Since indoor optical channels are power limited rather than bandwidth limited, PPM schemes with $L_{PPM} > 2$ would be a desirable option.

C. DPIM

Though PPM provides the best power efficiency, further improvement in either bandwidth or power efficiencies can be achieved by removing the redundant empty slots after the pulse (see Fig. 1). The differential PPM (DPPPM) and DPIM [11] remove these

redundancies and also offer reduces system complexity by offering symbol synchronization in contrast to PPM. In DPIM, each block of M (= $\log_2 L$) data bits is mapped to one of L possible symbols, each different in length. Every symbol begins with a pulse, followed by a series of empty slots, the number of which is dependent on the decimal value of the block of data bits being encoded (see Fig.1). The average symbol length for DPIM L_{DPIM} is reduced compared to the PPM and assuming independent and identically-distributed (*iid*) random data, the average symbol length L_{DPIM} and the slot duration T_{s_DPIM} are given by:

$$L_{DPIM} = \frac{(2^M+1)}{2}, \quad (5)$$

$$T_{s\_DPIM} = \frac{T_b M}{L_{DPIM}}. \quad (6)$$

For distortionless channel, the slot error probability of DPIM P_{se_DPIM} is given by:

$$P_{se\_DPIM} = Q\left(\sqrt{\frac{1}{2}L_{DPIM}M}\,\frac{RP_{avg}\sqrt{T_b}}{\sqrt{N_0/2}}\right). \quad (7)$$

3. Fluorescent Light Interference Model

The background radiation both from the artificial and natural light can cause serious performance degradation in indoor OW links. A number of artificial light sources have difference interfering patterns and their characteristics and performance of OW under the constraints of the ALI is well studied and interested reader can refer [5-7]. In absence of the FLs driven by electronic ballasts, any modulation techniques with HPF provide satisfactory performance. However, in the presence of the FLI, the performance of the system even with a HPF is far from satisfactory at data rate < 10Mbps for OOK.

For FLs driven by electronic ballasts can be model using two electrical components of the photocurrent at the receiver, a high frequency $m_{high}(t)$ and a low frequency $m_{low}(t)$ components. Thus, the zero mean periodic photocurrent $m_{fl}(t)$ due to FL is given as [5]:

$$m_{fl}(t) = m_{low}(t) + m_{high}(t), \quad (8)$$

where

$$m_{high}(t) = \frac{I_B}{A_2}\sum_{j=1}^{22}\Gamma_j \cos\left(2\pi f_{high} j t + \theta_j\right), \quad (9)$$

$$m_{low}(t) = \frac{I_B}{A_1}\sum_{i=1}^{20}\begin{bmatrix}\Phi_i \cos(2\pi(100i-50)t+\varphi_i)\\ +\Psi_i \cos(2\pi 100 i t+\phi_i)\end{bmatrix}, \quad (10)$$

$$\Phi_i = 10^{(-13.1\ln(100i-50)+27.1)/20}, \qquad 1 \le i \le 20$$

$$\Psi_i = 10^{(-20.8\ln(100i)+92.4)/20}, \qquad 1 \le i \le 20$$

where Φ_i and Ψ_i are the amplitudes of the odd and even harmonics of 50 Hz mains signal, respectively, Γ_j and θ_j are the amplitude and phase of the harmonics, f_{high} is the electronic ballast switching frequency, and A_2 is the constant relating the interference amplitude to I_B. For detail description and all parameter values readers can referred to [5].

Considering a linear system, the error probability in the presence of the ALI can be calculated by separately treating the FLI and signal at the receiver and adding them. The sampled output at the output of the matched filter due to the OOK-NRZ signal is $RP_{avg}\sqrt{T_b}$ for binary '1' and 0 for binary '0'. The output of the matched filter due to the FLI signal, sampled at the end of each bit period, is given as:

$$m_k = m_{fl}(t) \otimes r(t)\big|_{t=kT_b}, \quad (11)$$

where the symbol $\otimes$ denotes convolution. The sample output in the presence of the FLI is given by sum of these two signals. By considering every slot over a 20 ms interval (i.e. one complete cycle of $m_{fl}(t)$) and averaging, the P_{be_OOK} in presence of the AWGN is given by:

$$P_{be\_OOK} = \frac{1}{N}\sum_{k=1}^{N} Q\left(\frac{RP_{avg}\sqrt{T_b}+m_k}{\sqrt{N_0/2}}\right) + Q\left(\frac{RP_{avg}\sqrt{T_b}-m_k}{\sqrt{N_0/2}}\right), \quad (12)$$

where N is the total number of slots under consideration. By following similar approach, the slot error probabilities for PPM and DPIM can be calculated and for the details refer [8, 12].

4. DWT

The concept of the wavelet transform originated from short-coming of the Fourier transform to provide time-frequency resolution. The continuous wavelet transform (CWT) provides the time-frequency mapping of the signal to be analysed. The CWT is similar to the Fourier transform where an arbitrary function of time can be represented by an infinite summation. However the analysing functions are different. In wavelet analysis sinusoidal functions in the Fourier transform are replaced with the wavelet functions [13]. The signal is analysed by scaling and translating the wavelet functions known as the mother wavelet. Though CWT can provide good resolution in terms of time and frequency, the analysed signal have very high redundancy and the algorithm is a computationally demanding. The solution is to use the dyadic translation and scale rather than the continuous which give rise to faster algorithm: the DWT. DWT can be realized by using iterative filtrations known as the subband coding as shown in Fig. 2. The filter bank consists of a series of

lowpass $h(n)$ and highpass $g(n)$ filters, which satisfies the condition of a quadrature mirror filter. The DWT is computed by successive lowpass and highpass filtering and downsampling by 2 to give the approximation and details coefficients. The outputs at the first stage of the decomposition is given by [14]:

$$y_{1h}(k) = \sum_n x(n) \,.\, g(2k-n), \quad (13)$$
$$y_{1l}(k) = \sum_n x(n) \,.\, h(2k-n). \quad (14)$$

The second stage divides the lowpass band signal y_{1l} further to the lowpass y_{2l} and bandpass y_{2h}. The filtering and decimation process is continued until the required level is reached. This results in a logarithmic set of bandwidths as shown in Fig. 3. The reconstruction process is simply the inverse of the decomposition. Since the reconstruction and decomposition filters are same, the reconstructed signal can be approximated as:

$$x'(n) = \sum_k \big(y_{kh}(k).\, g(2k-n)\big) + \big(y_{\mathrm{kl}}(n).\, h(2k-n)\big). \quad (15)$$

5. System Descriptions

The proposed system block diagram for the OOK receiver based on the wavelet denoising is shown in Fig. 4. For the modulation techniques other than OOK, additional blocks of encoder and decoder at the transmitter and receiver is added to convert signal to the require format. The output of the optical transmitter is also scaled accordingly to make the average transmitted optical power to be P_{avg}. However, the working principle of the receiver remains the same. In addition to the ALI, signal independent shot noise $n(t)$ is added to the system to take account of the background radiations. The receiver fronts-end consists of a photodetector of responsivity R followed by a matched filter $r(t)$. The output of the matched filter $y(t)$ is sampled and the sampling frequency depends on the bit/slot rate as explained in previous sections. The sampled output $y(n)$ is further processed using the wavelet denoising and the denoised signal is converted into the binary data format

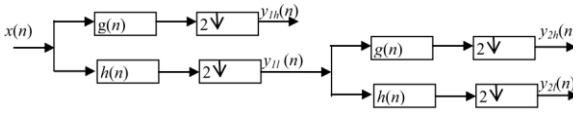

Fig.2. The DWT tree.

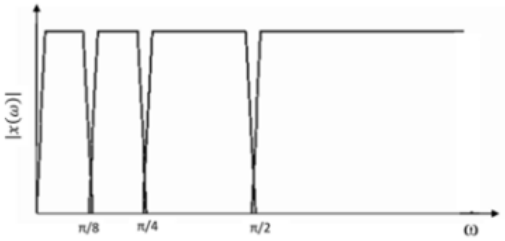

Fig.3. Frequency band of analysis tree.

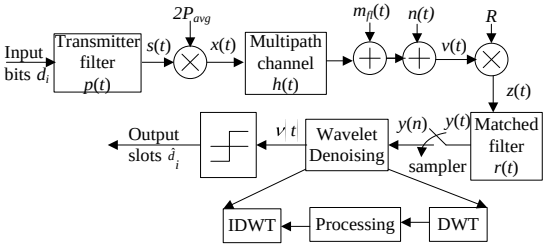

Fig.4. Proposed OW receiver for the OOK in presence of ALI.

using a threshold detector.

The wavelet denoising involves the decomposition of the signal $y(n)$, processing the DWT coefficients and reconstruction. $y(n)$ is decomposed into different bands using the DWT. The decomposition is carried out till the signal and interference is effectively separated from each other. Since the FLI is a low frequency band signal, the approximation coefficients need to be manipulated. For denoising proposes, the approximation coefficients corresponding to the FLI are then made equal to zero so that reconstructed signal is free from FLI, i.e.

$$y_{nh}(k) = 0. \quad (16)$$

where n is the decomposition level. The signal is then reconstructed using the inverse DWT as given by (15).

6. Results and Discussions

The computer simulations of the proposed system are carried out using Matlab for OOK, 8-PPM and 8-DPIM. As explained in previous section, DWT decomposes the signal in the logarithmic scale; therefore it is difficult to define a precise band of frequency that corresponds to the lowest level of approximations. The decomposition level is calculated in such a way that the lowest level of approximation signal is within 0.5 MHz range to make the cut-off frequency f_c approximately 0.5 MHz. The cut-off frequency is chosen as 0.5 MHz as previous studies showed that it provide near optimal performance in presence of FLI [15]. The decomposition level and approximated f_c at different data rate is given in Table I. The number of decomposition level K is calculated using the following expressions:

$$K = -\lceil \log_2(T_s \times 0.5\mathrm{E}6) \rceil, \quad (17)$$

where $\lceil x \rceil$ is the ceiling function. It is to be noted here that f_c varies with the data rate and the level of decompositions. Other key simulation parameters are given in Table II.

The PSD of the signal of OOK at 2 Mbps corrupted by FLI and its denoised version using DWT are shown in Fig. 5. The Daubechies wavelet (Db8) is used for the analysis with 6 levels of decompositions and the photocurrent due to interference is arbitrarily made four

Table I: The decomposition level *K* and the approximate cut-off frequency fc (MHz)

Data Rate (Mbps)	OOK		8-PPM		8-DPIM	
	K	f_c	***K***	f_c	***K***	f_c
10	5	0.31	6	0.42	5	0.47
20	6	0.31	7	0.42	6	0.47
40	7	0.31	8	0.42	7	0.47
60	7	0.47	9	0.31	8	0.35
80	8	0.31	9	0.42	8	0.47
100	8	0.39	10	0.26	9	0.29
120	8	0.47	10	0.31	9	0.35
140	9	0.27	10	0.36	9	0.41
160	9	0.31	10	0.42	9	0.47
180	9	0.35	10	0.47	10	0.26
200	9	0.39	11	0.26	10	0.29

Table II: The simulation parameters

Parameters	Value
Data rate R_b	10-200 Mbps
Modulation types	OOK, PPM, DPIM
Bit Resolution	3
Mother wavelet	'Db8'
Photodetector responsivity *R*	1
Background radiation current	200 µA
Data rate R_b	10-200 Mbps
Bit Resolution	3
Mother wavelet	'Db8'

times that of the signal. The signal is assumed to be free from the AWGN for the PSD calculations. However, in all other simulations, the background shot noise is included. The PSD diagram of the denoised signal shows that there are no significant changes in PSD at frequency > 0.5 MHz compared to the PSD of the original signal. Significant portion of the spectral content at < 0.3 MHz is removed (the approximated cut-off frequency is 0.31 MHz) with no DC contents. Because of the spectral overlap between signal and interference (both having high DC and low frequency components), it is not possible to remove the interference without losing significant portion of signal, thus leading to a power penalty. Hence the task here is to make the power penalty as low as possible. With this observation, one can conclude that the signal with low PSD at or near the DC value can provide enhanced immunity to the FLI.

The normalized optical power penalties (OPP) for OOK, 8-PPM and 8-DPIM for ideal and interfering channels and with DWT denoising at data rate of 10 - 200 Mbps are depicted in Fig. 6. The OPP is normalized to the power required to achieve an error rate of 10^{-6} in an ideal channel for OOK at 1 Mbps. The OPP associated with FLI without filtering is not studied here, since it has been reported in the literature. The OPP in presence of the FLI with DWT is the highest for OOK with 8-DPIM and 8-PPM showing much improved performance. The OPP for OOK in the presence of FLI compared to ideal channel decreases with increasing

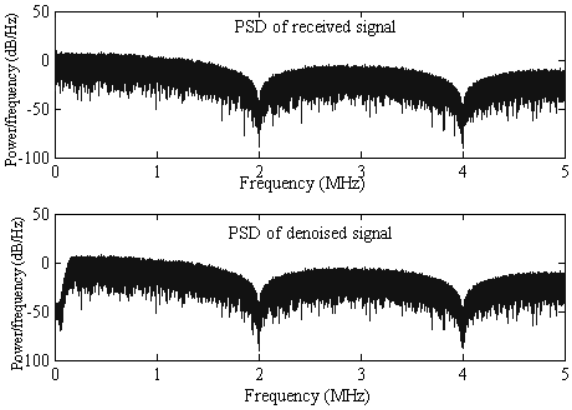

Fig.5. The power spectral density (PSD) of OOK at 2 Mbps: (a) with FLI and (b) with DWT. The Daubechies wavelet is used for analysis with 6 levels of decompositions.

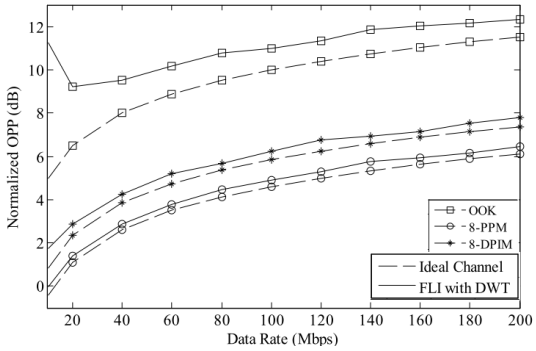

Fig. 6. Normalized OPP to achieve a error rate of 10^{-6} for OOK, 8-PPM and 8-DPIM for ideal and interfering channels and with DWT denoising at data rate of 10 - 200 Mbps.

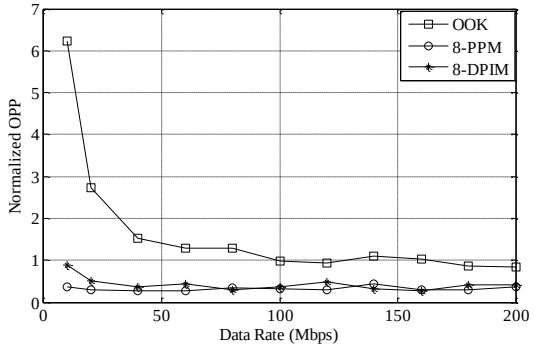

Fig. 7: The normalized OPP to achieve a error rate of 10^{-6} for OOK, 8-PPM and 8-DPIM for ideal and interfering channels and with DWT denoising at data rates of 10 - 200 Mbps.

date rate. Clearly, PPM and DPIM display more resilience to the FLI.

Further insight can be achieved by calculating the difference of the OPP for the ideal and non-ideal (in presence of FLI) channels with other parameters (modulation type, data rate) being kept the same. The normalized OPP for OOK, 8-PPM, and 8-DPIM is shown in Fig. 7. Unlike in Fig. 6, OPP is the normalized

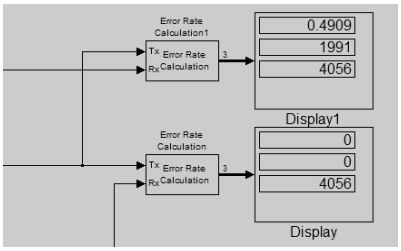

Fig.8. BER performance OOK in presence of the FLI with and without DWT denoising. DWT denoising is performed using TMS320C6713.

to the power required to achieve an error rate of 10^{-6} in an ideal channel for identical data rate and modulation type. The OPP is highest and lowest for OOK and PPM, respectively. This is because OOK has a high DC component which is removed while denoising. For OOK, the OPP is rather high for data rates < 40 Mbps and for data rates > 40 Mbps, it is almost 1 dB. Both PPM and DPIM show very similar performance with the latter displaying ~0.5 dB higher OPP at 10 Mbps compared to PPM. Since the power spectral density of DPIM has non-zero DC values, it provides inferior performance compared to the PPM. However, the DC component in DPIM is much smaller compared to the DC component of OOK [8], and hence providing much improved performance.

The proposed system is practically implemented using the TMS320C6713 DSP board. For the verification, rapid prototyping using the Simulink and RTDX are carried out. For the comparative studies, the outputs of the denoising module from Matlab and DSP are compared showing a very low error (in range of 10^{-12}) between the signals. The error rate for OOK system in presence of FLI with/without DWT is calculated and a snapshot is illustrated in Fig. 8, showing error free performance, thus confirming the validity of the proposed system.

7. Conclusion

An alternative approach of reducing the FLI for indoor OW channel using the discrete wavelet transform is investigated in this paper. The signal and interference are separated in wavelet domain and the interference is removed from the received signal. The denoised signal is used for recovering the binary digit using a threshold detector. The proposed system was simulated for different baseband modulation techniques for LOS OW links. The results show that the DWT is very effective in reducing interference in OW receiver. Comparative studies with the performance in ideal channel show that modulation technique like OOK with high spectral contents at/near DC values offers the least desirable performance even with denoising. On the other hand, power penalty for PPM and DPIM is less than 0.5 dB with DWT denoising. The proposed system was practically realized using DSP and the results also confirmed the validity of proposed system.

REFERENCES

[1] N. Cvijetic, D. Qian, and T. Wang, "10Gb/s Free-Space Optical Transmission using OFDM," in *Conference on Optical Fiber communication/National Fiber Optic Engineers Conference, 2008*, San Diego, CA, 2008, pp. 1-3.

[2] F. Marioni, Z. Sodnik, and F. E. Zocchi, "2.5-Gb/s free-space optics link over 1.1 km with direct fiber coupling to commercial devices," *Proceedings of the SPIE*, vol. 5550, pp. 60-69, 2004.

[3] R. D. Wisely, "A 1 Gbit/s optical wireless tracked architecture for ATM delivery," in *IEE Colloquium on Optical Free Space Communication Links*, London, UK, 1996, pp. 14/1-14/7.

[4] J. M. Kahn and J. R. Barry, "Wireless infrared communications," *Proceedings of IEEE*, vol. 85, pp. 265-298, 1997.

[5] A. J. C. Moreira, R. T. Valadas, and A. M. d. O. Duarte, "Optical interference produced by artificial light," *Wireless Networks*, vol. 3, pp. 131-140, 1997.

[6] R. Narasimhan, M. D. Audeh, and J. M. Kahn, "Effect of electronic-ballast fluorescent lighting on wireless infrared links," *IEE Proceedings - Optoelectronics*, vol. 143, pp. 347-354, 1996.

[7] A. J. C. Moreira, R. T. Valadas, and A. M. d. O. Duarte, "Performance of infrared transmission systems under ambient light interference," *IEE Proceedings -Optoelectronics*, vol. 143, pp. 339-346, 1996.

[8] Z. Ghassemlooy, "Investigation of the baseline wander effect on indoor optical wireless system employing digital pulse interval modulation," *IET Communications*, vol. 2, pp. 53-60, 2008.

[9] J. R. Barry, *Wireless Infrared Communications*. Boston: Kluwer Academic Publishers, 1994.

[10] K. K. Wong, T. O'Farrell, and M. Kiatweerasakul, "The performance of optical wireless OOK, 2-PPM and spread spectrum under the effects of multipath dispersion and artificial light interference," *International Journal of Communication Systems*, vol. 13, pp. 551-57, 2000.

[11] Z. Ghassemlooy and A. R. Hayes, "Digital pulse interval modulation for IR communication systems-a review," *International Journal of Communication Systems*, vol. 13, pp. 519-536, 2000.

[12] A. R. Hayes, "Digital pulse interval modulation for indoor optical wireless communication systems," PhD thesis, Sheffield Hallam University, UK, 2002.

[13] C. M. Leavey, M. N. James, J. Summerscales, and R. Sutton "An introduction to wavelet transforms: a tutorial approach," *Insight*, vol. 45, pp. 344-353, 2003.

[14] C. S. Burrus, R. A. Gopinath, and H. Guo, *Introduction to wavelets and wavelet transforms: A primer* New Jersey: Prentice Hall, 1998.

[15] R. J. Dickenson, "Wavelet analysis and artificial intelligence for diffuse indoor optical wireless communication", PhD thesis, Northumbria University, UK, 2007.